International journal of applied and computational mathematics.

MAHABALESHWAR, U.S., MAHESH, R. and CHAN, A.

2024

Int. J. Appl. Comput. Math (2024) 10:47
https://doi.org/10.1007/s40819-024-01685-w

ORIGINAL PAPER

Stagnation-Point Brinkman Flow of Nanofluid on a Stretchable Plate with Thermal Radiation

U. S. Mahabaleshwar[1] · R. Mahesh[1] · A. Chan[2]

Accepted: 12 January 2024

Abstract
The study is an analytical exploration of hybrid nanofluid flow at a stagnation-point with Brinkman effect on a stretchable plate with thermal radiation. All of the aforementioned factors were taken into account when developing the mathematical model based on the Navier–Stokes equations for nanofluids, leading to a system of partial differential equations. Using suitable scaling, these equations are reduced to system of ordinary differential equations. The outcome of the system of ordinary differential equations are solved analytically and closed-form solutions are obtained in terms of incomplete error function. The results are analysed for the many significant flow characteristics with the profiles of velocity and temperature explored graphically. The amount of the heat transfer is increased due to the interaction between nanoparticles and the wall, and the wall surface is cooled when wall suction is present.

Keywords Brinkman ratio · Hybrid nanoparticles · Thermal radiation · Stagnation point

Introduction

Nanofluids are known as a type of fluid suspended with 100 nm or smaller carbon nanotubes or oxide nanoparticles which is initially discovered by the Choi [1]. Later, several researchers contributed to their work on the nanofluids like Makinde [2] and Hayat et al. [3]. The word hybrid nanofluid (HNF) refers to the combination of two different types of nanofluids which has a thermophysical characteristics that aids in regulating the rate of heat transfer and is appropriate for a variety engineering applications. Several researchers looked at HNF flow across various surfaces as a result of these characteristics. Water-based HNF flow in a porous

✉ A. Chan
a.chan5@rgu.ac.uk

U. S. Mahabaleshwar
u.s.m@davangereuniversity.ac.in

R. Mahesh
maheshrudraiah15@gmail.com

1 Department of Studies in Mathematics, Shivagangotri Davangere University, Davangere, India

2 School of Engineering, Robert Gordon University, Aberdeen AB10 7GJ, UK

Published online: 16 February 2024

channel with entropy production was investigated by Das et al. [4]. Anusha et al. [5] showed the effect of the HNF on an unsteady stagnation point of non-Newtonian fluid. Aly et al. [6] studied the wall jet flow on a suction/injection with thermal radiation. Mahabaleshwar et al. [7] examined the effect of HNF on a Newtonian fluid. Recently Poornima [8] investigated the effect of CuO + MgO nanoparticles on a stagnation point flow (SPF) of over a stretching/contraction cylinder. The fluid flow near stagnation point on stretching/shrinking sheet with MHD, partial slip and viscous dissipation on heat transformed was investigated by the Aly and Pop [9], and later on by Shatanawi et al. [10], Jamaludin et al. [11], Anuar et al. [12] along similar directions.

A region in the flow field where the fluid particles have vanishing velocity from all directions is referred to as the stagnation point. When a body is lying in the flow field, this stagnation point often occurs at the surface of the body. Engineering solutions to these stagnation point flow (SPF) problems are sought for use in aeroplanes, nuclear reactors, electronic appliance coolants, wire and plastic sheet drawing or polymer extraction. Along this line of application, the idea of non-Newtonian fluids flowing across a stretchy plate near their stagnation point was first explained by Hiemenz [13]. As a continuation of this work, Wu et al. [14], Weidman and Mahalingam [15], and Stuart [16] are works credited as leading investigations. The Cattaneo-Christov heat flux model was used by Hayat et al. [17] to analyse the effects of SPF on a nonlinear stretched surface. Other writers, including Meraj et al. [18], Bhattacharya et al. [19], Merkin and Pop [20], Zhang et al. [21], and recently, Mahabaleshwar et al. [22], have been actively deliberating the study of SPF taking into account various physical characteristics of applications.

The present work is carried with heat radiation and Brinkman ratio between the two fluid components which has been studied by many researchers like Hsu et al. [23], Sneha et al.[24], Zhao et al. [25], Anusha et al. [26]. The impact of thermal radiation of HNF is crucial in the fields of solar energy, astrophysical fluxes and energy production. According to Bestman and Adjepong [27], thermal radiation influences are crucial to the structure of high-temperature flow processes. The effect of heat radiation on boundary layer movement has been extensively covered in the present body of knowledge. To give an example, the thickness of the thermal boundary layer rises with an increase in radiation parameter, according to Sajid and Hayat's [28] investigation on the impact of thermal radiation on the viscous flow on an exponentially stretchable sheet. The work by Sneha et al. [29], Lund et al. [30], and Maranna et al. [31] explored how thermal radiation impacts heat transfer rate. The SPF of the non-Newtonian fluid was presented by Lund [32] with radiation on an expanding/contracting sheet. Khan et al. [33] inspected how thermal radiation effects on SPF.

The present investigation is an extension work of Turkyilmazoglu [34]. The novelty of the present investigation describes the behaviour of a mixture of nanofluids with a certain Brinkman ratio near a stretchable flat surfaces with thermal radiation. This work seeks application in aerodynamic, nuclear reactors, electronic appliance coolants and other industrial application. In spite of the aforementioned studies, this has not been accomplished up to now. Exact form solutions of the SPF are offered in accordance with this objective. Analytical solution of the resulting thermal field also produces exact formulations for the thermal field and heat transfer rate is calculated from the object immersed into the fluid.

Mathematical Formulation and Solution

We consider the two-dimensional stagnation point flow arising from an axial velocity of $u = U(x) = cx$ of hybrid nanofluid with a Brinkman ratio on a stretchable plate with

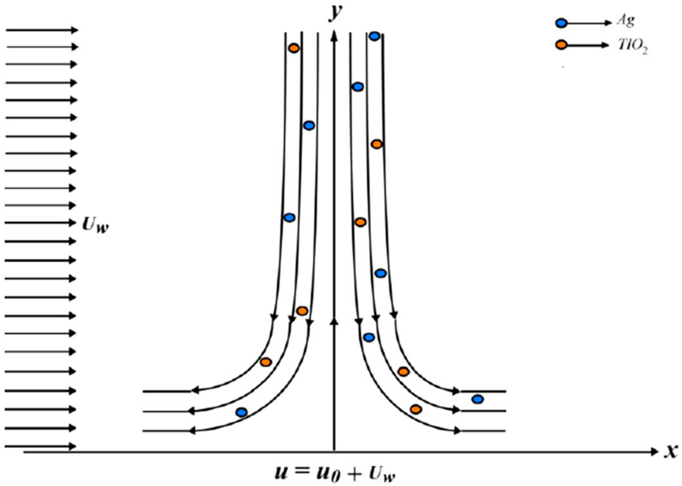

Fig.1 The flow development in Cartesian coordinate system

thermal radiation. The velocity of the stretching surface is considered as $u = U(x) + u_0$ where u_0 is the constant velocity as shown in Fig. 1, with axis $'x'$ and $'y'$ represented by the velocity components (u, v) in this case. Also keep in mind that the system's axial and radial coordinates affect the pressure 'p'. Additionally, only constant wall temperatures T_w and ambient temperatures T_∞ are related to temperature in terms of radial coordinates. The coordinate system in Cartesian and cylindrical forms is used to study solution brinkman ratio of the defined phenomenon in two dimensions. As a result, the following equations serve as the governing equations for the aforementioned flow (see [34]).

The governing system of equations for the Cartesian coordinate system as follows

$$\frac{\partial u}{\partial x} + \frac{\partial v}{\partial y} = 0 \tag{1}$$

$$u\frac{\partial u}{\partial x} + v\frac{\partial u}{\partial y} = -\frac{1}{\rho_{hnf}}\frac{\partial p}{\partial x} + \frac{\mu_{eff}}{\rho_{hnf}}\left(\frac{\partial^2 u}{\partial x^2} + \frac{\partial^2 u}{\partial y^2}\right) \tag{2}$$

$$u\frac{\partial v}{\partial x} + v\frac{\partial v}{\partial y} = -\frac{1}{\rho_{hnf}}\frac{\partial p}{\partial y} + \frac{\mu_{eff}}{\rho_{hnf}}\left(\frac{\partial^2 v}{\partial x^2} + \frac{\partial^2 v}{\partial y^2}\right) \tag{3}$$

$$u\frac{\partial T}{\partial x} + v\frac{\partial T}{\partial y} = \alpha_{hnf}\frac{\partial^2 T}{\partial y^2} - \frac{1}{\left(\rho C_p\right)_{hnf}}\frac{\partial q_r}{\partial y}, \tag{4}$$

The boundary conditions are

$$\begin{cases} U(y=0) = u_0,\ U(y\to\infty) = \frac{\beta_1 \nu_{hnf}^2}{a} \\ T(y=0) = T_w,\ T(y\to\infty) = T_\infty, \end{cases} \tag{5}$$

It should be noted that the thermal and hydrodynamic parameters are assumed to be constant and independent of any external factors. Using the aforementioned reasonable hypotheses, the axial velocities in can be represented as follows

$$\begin{cases} u = U(x) + U(y), \\ v = -ay - v_0, \end{cases} \tag{6}$$

Table 1 Thermal properties of base fluid and hybrid nanofluid (See [36])

physical properties	Ag	TIO_2	Fluid phase (water)
$C_p\,(\mathrm{J/Kg\,K})$	235	686.2	4179
$\rho\left(\mathrm{Kg/m^3}\right)$	10,500	4250	997.1
$\kappa\,(\mathrm{W/mK})$	429	8.9528	0.613
$\sigma\,(\Omega/\mathrm{m})^{-1}$	62.1×10^6	2.6×10^6	0.05

The stretching flow via v_0 in Eq. (11) makes a net rate of suction or injection achievable over a flat surface. Moreover, under the potential flow provided by the Eq. (5–8), the stagnation-point flow occurs (12). It is also crucial to be aware of the pressure being applied to the flow. The following is said to be the flat plate pressure solution (see [34])

$$p=-\rho_{hnf}\left(\frac{a^2}{2}\left(x^2+y^2\right)+a\,v_0y+\beta_1\nu_{hnf}^2x-p_0\right), \tag{7}$$

where β_1 and p_0 are constants.

Expressions and Thermophysical Properties of the Hybrid Nanofluid

$$\begin{cases} A=\dfrac{\mu_{hnf}}{\mu_f}=\dfrac{1}{(1-\varphi_1)^{2.5}(1-\varphi_2)^{2.5}},\\ A_2=\dfrac{\rho_{hnf}}{\rho_f}=(1-\varphi_2)\left(1-\varphi_1+\varphi_1\dfrac{\rho_{s1}}{\rho_f}\right)+\varphi_2\left(\dfrac{\rho_{s2}}{\rho_f}\right),\\ A_3=\dfrac{\left(\rho C_p\right)_{hnf}}{\left(\rho C_p\right)_f}=(1-\varphi_2)\left(1-\varphi_1+\varphi_1\left(\dfrac{\left(\rho C_p\right)_{s1}}{\left(\rho C_p\right)_f}\right)\right)+\varphi_2\left(\dfrac{\left(\rho C_p\right)_{s2}}{\left(\rho C_p\right)_f}\right),\\ A_4=\dfrac{\kappa_{hnf}}{\kappa_f}=\dfrac{\kappa_{s2}+2\kappa_{bf}+2\varphi_2\left(\kappa_{s2}-\kappa_f\right)}{\kappa_{s2}+2\kappa_{bf}-\varphi_2\left(\kappa_{s2}-\kappa_f\right)},\quad where\quad \kappa_{bf}=\kappa_f\dfrac{\kappa_{s1}+2\kappa_f+2\varphi_1\left(\kappa_{s1}-\kappa_f\right)}{\kappa_{s1}+2\kappa_f-\varphi_1\left(\kappa_{s1}-\kappa_f\right)}, \end{cases} \tag{8}$$

where C_p is the specific heat capacity. $\rho_{s1},\ \rho_{s2},\ \kappa_{s1},\ \kappa_{s2}\,and\,\kappa_{bf},\ \rho_{bf}$ are the density and thermal conductivities of nanoparticles of TIO_2 and Ag and base fluid H_2O. φ_1 and φ_2 are the solid volume fraction of nanoparticles of TIO_2 and Ag respectively. The thermophysical values of the respective HNF properties are listed in Table 1

Analytical Solutions for Momentum Equations

The simplified form of the axial velocity is obtained as follows by using the Eqs. (6–8)

$$\frac{\Lambda\,\nu_f}{A_2}\frac{d^2U(y)}{dy^2}+(a\,y+v_0)\frac{dU(y)}{dy}-aU(y)=-\beta_1\,\nu_{hnf}^2, \tag{9}$$

with boundary conditions

$$U(y=0)=u_0,\quad U(y\to\infty)=\frac{\beta_1\,\nu_{hnf}^2}{a}, \tag{10}$$

The asymptotic characteristics of velocity is the cause of the second boundary condition in Eq. (10). Moreover, using the scaled quantities listed below, the dimensionless mode solution for Eq. (9) is obtained:

$$\widehat{U} = \frac{U}{\frac{\nu_{hnf}}{L}}, \quad \widehat{v} = \frac{v}{\frac{\nu_{hnf}}{L}}, \quad \widehat{x} = \frac{x}{L}, \quad \widehat{y} = \frac{y}{L}, \quad \widehat{p} = \frac{L^2}{\nu_{hnf}^2 \rho} p, \tag{11}$$

The reference scale length in this case is L. Equation (9) is changed into the following equation by using these scaling:

$$\frac{d^2(U(y))}{dy^2} + (Ay + s)\left(\frac{A_2}{\Lambda}\right)\frac{d(U(y))}{dy} - A\left(\frac{A_2}{\Lambda}\right)U(y) = -\beta\left(\frac{A_1}{\Lambda}\right), \tag{12}$$

with associated boundary conditions

$$U(y = 1) = u_0, \quad U(y \to \infty) = \frac{\beta}{A}\left(\frac{A_1}{A_2}\right). \tag{13}$$

As you can see, $A = \frac{aL^2}{\nu_f}$ known as stretching parameter, the permeability parameter is known by $s = \frac{v_0 L}{\nu_f}$, and the pressure parameter $\beta = \beta_1 L^3$,

The stretchable flow across a flat plate is evaluated using Eq. (12), and the axial velocity is expressed as an incomplete error function given in the Eq. (14).

$$U(y) = \frac{1}{D}\left\{\begin{array}{l} Exp\left[-\frac{(s+Ay)^2 A_2}{2A\Lambda}\right]\left(-2\sqrt{A\Lambda}\left(Au_0 + \left(Exp\left[-\frac{(s+Ay)^2 A_2}{2A\Lambda}\right] - Exp\left[\frac{s^2 A_2}{2A\Lambda}\right]\right)\beta\left(\frac{A_1}{A_2}\right)\right)\right) \\ +Exp\left[\frac{s^2 A_2}{2A\Lambda}\right]\sqrt{2\pi A_2}\left(S\beta\left(\frac{A_1}{A_2}\right)Erfc\left[\frac{s\sqrt{A_2}}{\sqrt{2A\Lambda}}\right] + (s+Ay)\left(u_0 A - \beta\left(\frac{A_1}{A_2}\right)\right)Erfc\left[\frac{(s+Ay)\sqrt{A_2}}{\sqrt{2A\Lambda}}\right]\right) \end{array}\right\}, \tag{14}$$

where $D = -2A^{\frac{3}{2}}\sqrt{\Lambda} + \sqrt{2\pi A_2}As\, Exp\left[-\frac{s^2 A_2}{2A\Lambda}\right]Erfc\left[\frac{s}{\sqrt{2A\Lambda}}\right]$,

Exact Solutions for Heat Equation

Temperature at and far from the body surfaces is assumed to be constant, as stated in the earlier section. As a result, in the flow field, the temperature of the flow is taken into account vertically. Thus, temperature equations in Eq. (4) and Eq. (8) are simplified as:

$$-(ay + v_0)\frac{\partial T}{\partial y} = \alpha\frac{\partial^2 T}{\partial y^2} - \frac{1}{(\rho C_p)_{hnf}}\frac{\partial q_r}{\partial y}, \tag{15}$$

with

$$T(y = 0) = T_w, \text{ and } T(y \to \infty) = T_\infty. \tag{16}$$

The radiative heat flux q_r is estimated using Rosseland approximations as below (Rosseland [35])

$$q_r = -\frac{4\sigma * T_\infty^3}{3k*}\frac{\partial T^4}{\partial y} \tag{17}$$

T^4 is expanded by Using Taylor series, and considered the expansion containing lower order $(T - T_\infty)$ terms, which results with, $T^4 \cong T_\infty^3(-3T_\infty + 4T)$.

Therefore, the radiative heat flux derivative is,

$$\frac{\partial q_r}{\partial y} = -\frac{16\sigma * T_\infty^3}{3\left(\rho C_p\right)_f \kappa_f} \frac{\partial^2 T}{\partial y^2}, \tag{18}$$

Using the scaling quantities in Eq. (8) and the transformation $\theta = \frac{T - T_\infty}{T_w - T_\infty}$, the thermal Eq. (15) are reduced to

$$(A_4 + Nr)\frac{d^2\theta}{dy^2} + Pr\, A_3\, (A\, y + s)\frac{d\theta}{dy} = 0 \tag{19}$$

with the corresponding conditions

$\theta(y = 0) = 1,$ and $\theta(y \to \infty) = 0.$and

Solving these equations, we get the thermal solutions as below:

$$\theta(y) = \frac{Erfc\left(\frac{\sqrt{Pr A_3}(Ay+s)}{\sqrt{2A(A_4+Nr)}}\right)}{Erfc\left(\frac{s\sqrt{Pr A_3}}{\sqrt{2A(A_4+Nr)}}\right)} \tag{20}$$

where $Nr = \frac{16\sigma^* T_\infty^3}{3k^* \kappa_f}$ and $Pr = \frac{\nu_f}{\alpha_f}$.

Result and Discussion

The present investigation is to obtain the analytical solution of a hybrid nanofluid flow in a stretching flat plate with effect Brinkman ratio with thermal radiation on the momentum and thermal boundary. The TIO_2 and Ag nanoparticles are consider and water acting as a base liquid. The value of Prandtl number (P_r) is fixed 6.2. It is significant to note that the data on the thermophysical properties of the fluid and nanofluid included in Table 1 and thermophysical expressions in (14) was used to calculate each nanofluid scenario. The impact of the physical parameter like A, S,Λ and N_r are discussed with help of graphs.

The demonstrates the normalised velocity distribution is affected by the stretching parameter A is and Brinkman ratio are show in the Fig. 2a, b. We observed that the stretching factor rises as velocity reductions for maintaining the values of the other parameters at $u_0 = 0$, s = 0, and $\Lambda = 1$. The asymptotic behaviour at infinity is realistic, and it is obvious that A has a dampening effect on the intensity of the momentum. We also observed that when strength A increased, the velocity boundary layer decreased. Figure 2b. Represents the normalised velocity distribution is affected by the Brinkman ratio parameter Λ. We observed that by increasing the value Λ the fluid velocity decreases.

The succeeding demonstration in Fig. 3a, b shows the appropriate patterns of the streamlines and vector field. As a result of the disparity in velocities between the horizontal surface and the very top, we see that an oblique stagnation occurs. By increasing the value of A (stretching parameter) an effect on streamlines and velocity fields as shown in the Figs. 4a, b and 5a, b the impact of larger value of A leads the orthogonal stagnation-point flow as shown in Fig. 2 which is cussed by the suppression of U. The vector and streamlines graphs for the effect of the suction and injection are demonstrated in Figs. 6a, b and 7a, b respectively streamlines and vector the concept of wall suction controls fluid flows which leads to the collision of the particular downstream locations. Furthermore, the radial location y = − s benefits from streamline divergence due to injection.

The impact of variables s and A on the temperature profile is seen in Fig. 8. It is obvious that

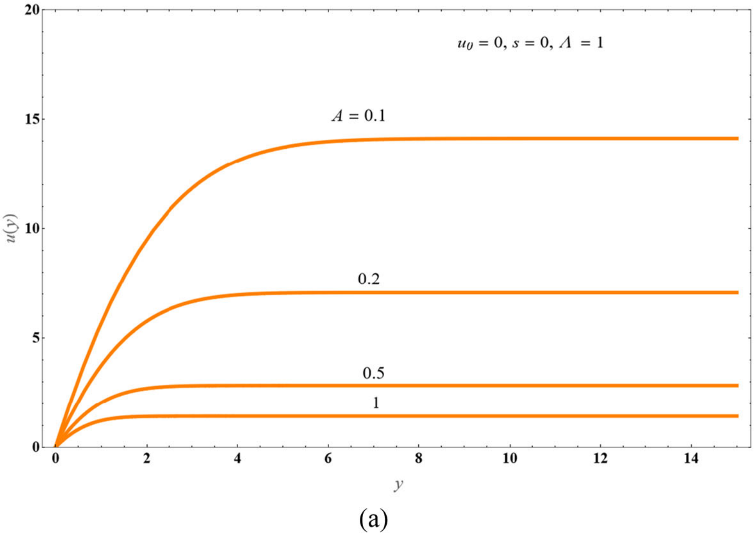

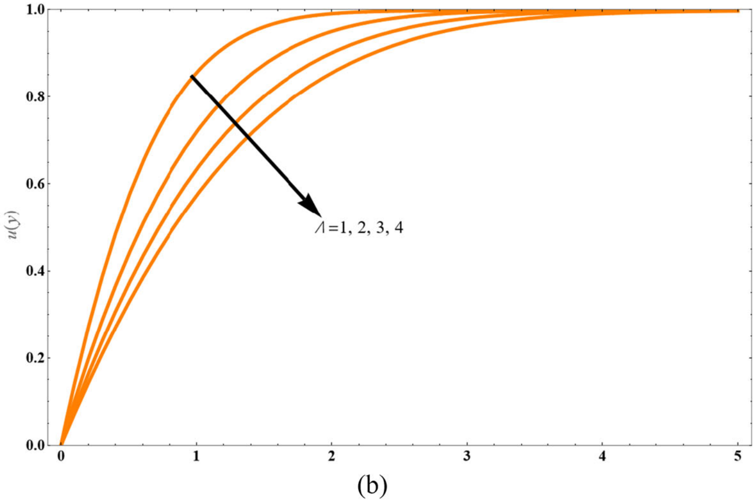

Fig. 2 The velocity distribution of **a** stretching parameter A and **b** Brinkman ratio

raising A has a cooling effect and causes the thermal layer's thickness to decrease. Compared to the rapid cooling that is a feature of wall suction, wall injection slows the cooling.

The influence of the flow's thermal radiation is shown in Fig. 9. It demonstrates that the heat energy discharged from the flow area as a consequence of a rise in the N_r causes a rise in the fluid temperature.

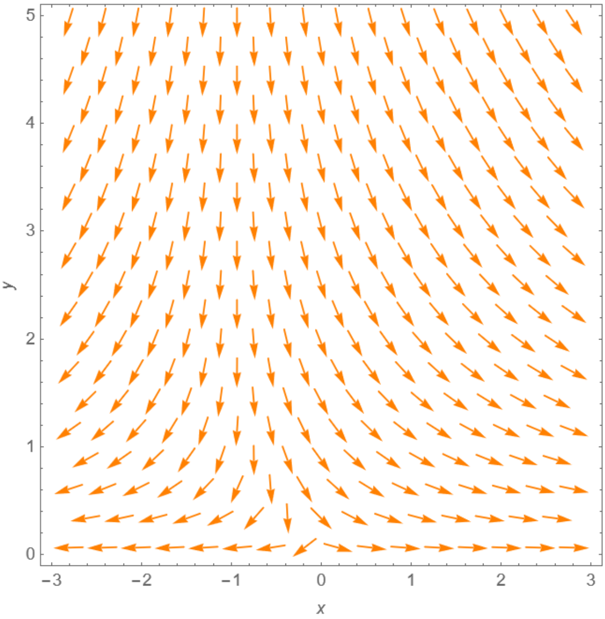

(a)

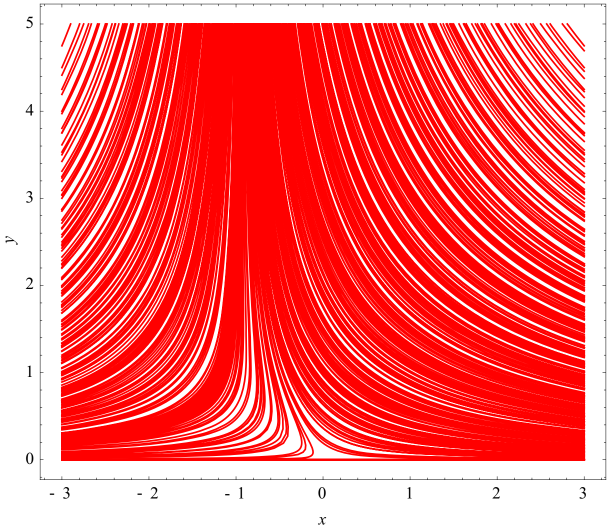

(b)

Fig. 3 Impact of $U_0 = s = 0$ $\Lambda = 1$ and $A = 1$ on **a** vector field and **b** Streamlines for

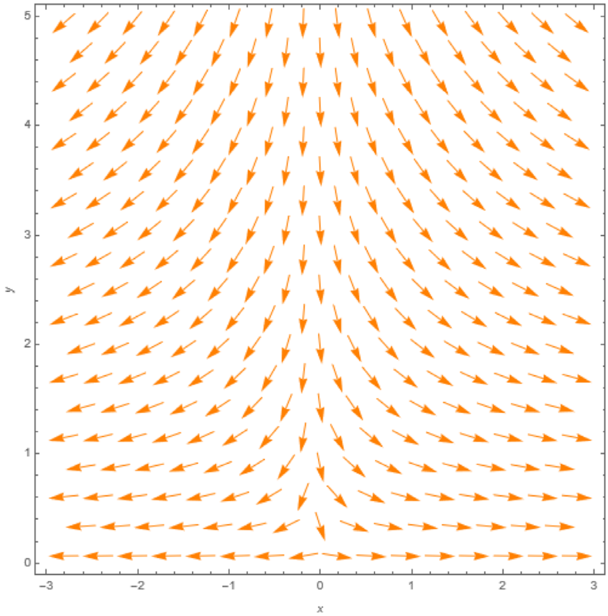

(a)

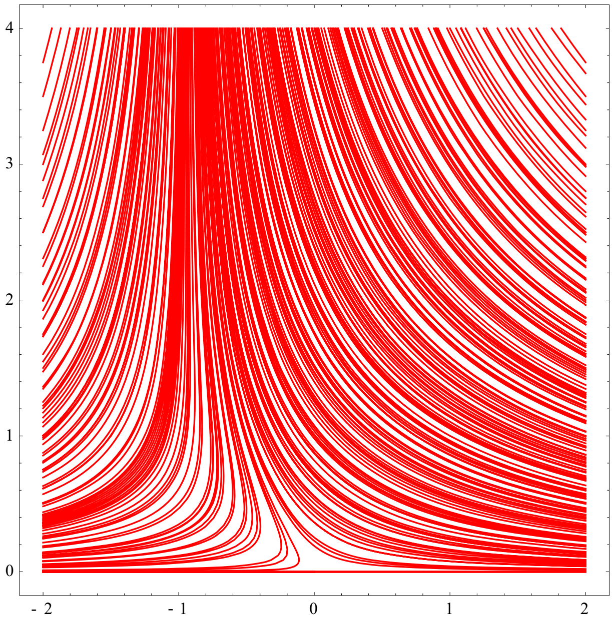

(b)

Fig. 4 Impact of stretching parameter when $U_0 = s = 0$ $\Lambda = 1$ and $A = 2$on **a** vector field and **b** Streamlines

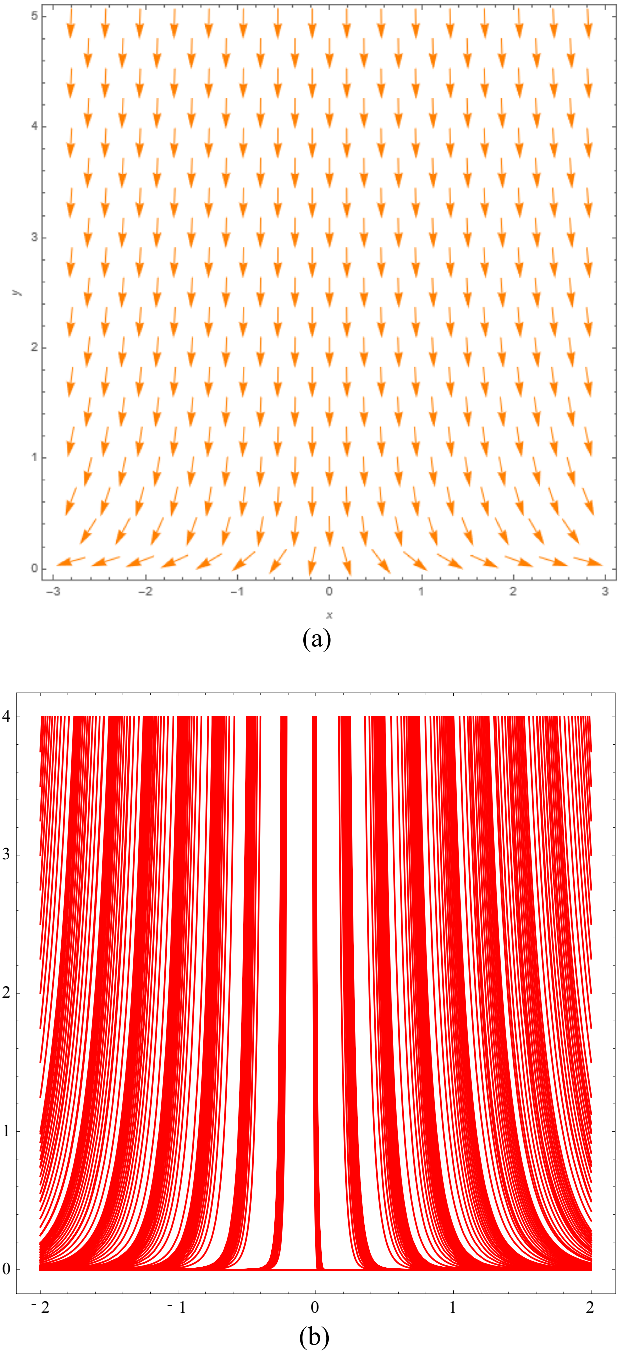

Fig. 5 Impact of stretching parameter when $U_0 = s = 0$ $\Lambda = 1$ and $A = 10$ on **a** vector field and **b** Streamlines

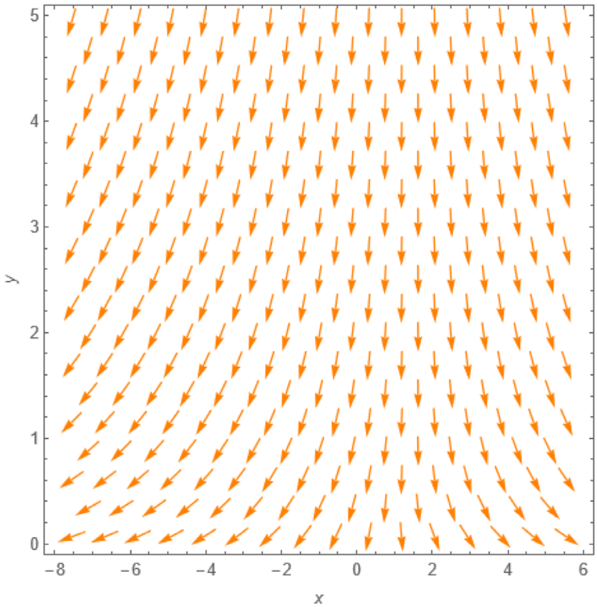

(a)

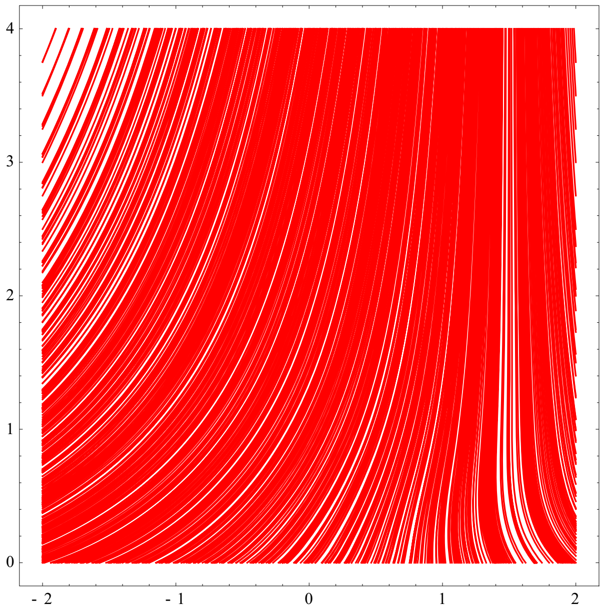

(b)

Fig. 6 impact of stretching parameter when $U_0 = 0$, $s = 0.5$ $\Lambda = 1$ and $A = 1$ on **a** vector field and **b** Streamlines

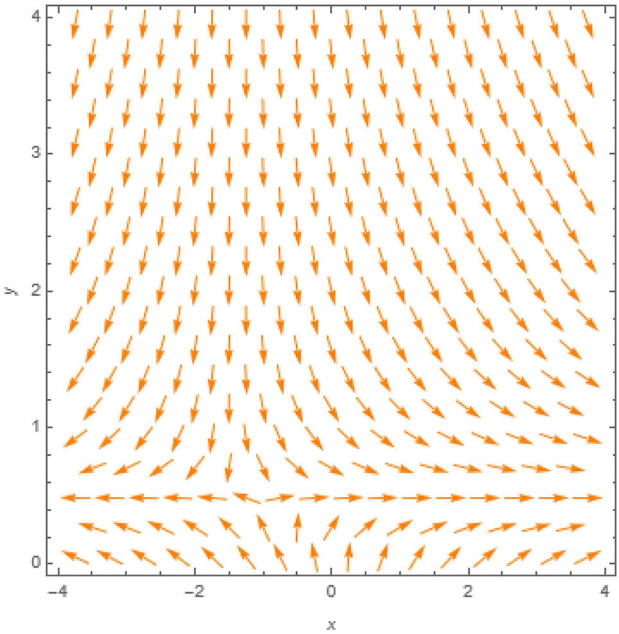

(a)

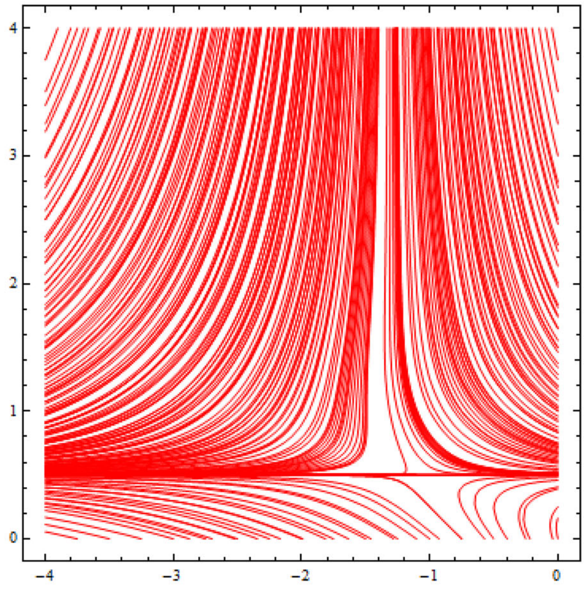

(b)

Fig. 7 Impact of stretching parameter when $U_0 = 0$, $s = 0.5$ $\Lambda = 1$ and $A = 11$on **a** vector field and **b** Streamlines

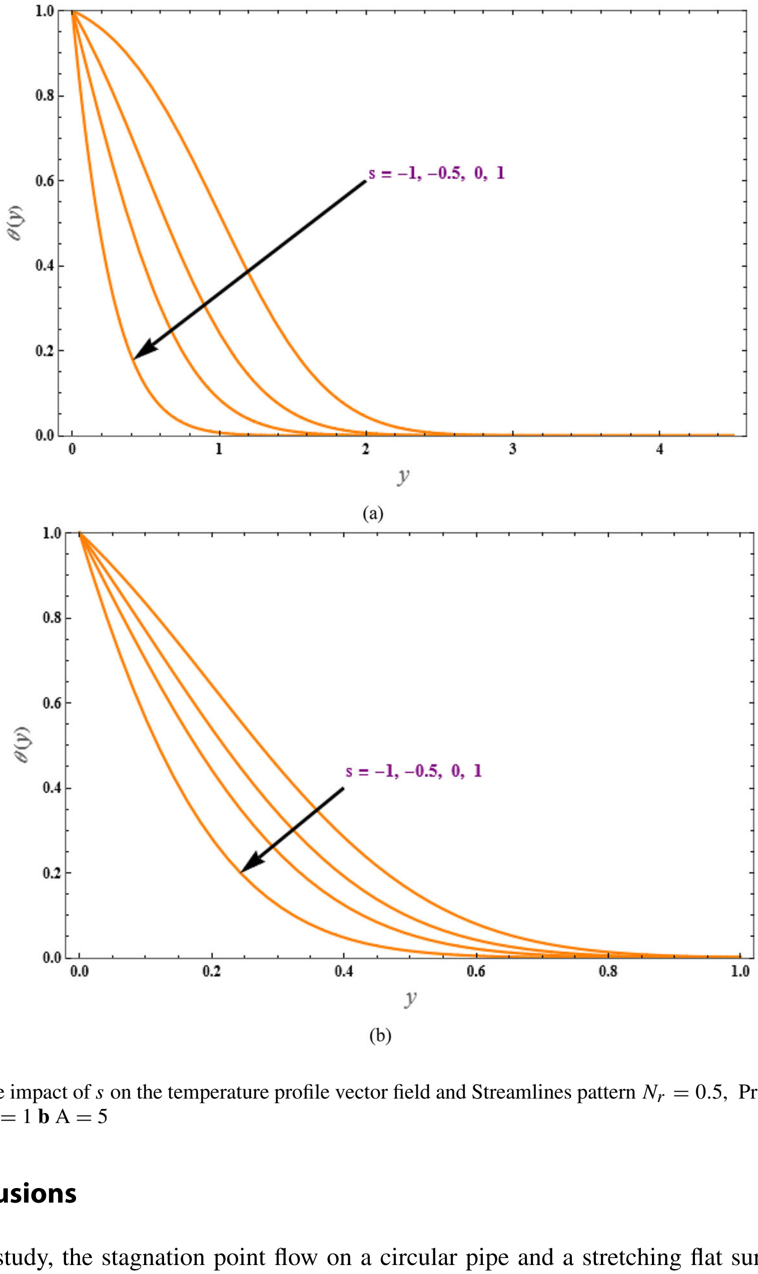

Fig. 8 The impact of s on the temperature profile vector field and Streamlines pattern $N_r = 0.5,\ \Pr = 6.2,\ \Lambda = 1$, **a** A = 1 **b** A = 5

Conclusions

In this study, the stagnation point flow on a circular pipe and a stretching flat surface are examined with the effect of brinkman ratio and heat transfer with thermal radiation with mass suction/injection is covered in the present study. In the absence of stretching, the walls are exposed to injection and suction in accordance with the exact solutions, which tends to the known specific constraints. The solutions lead to the following physical observations:

- The stretching surfaces have the effect of suppressing the flow's axial velocities. The stagnation-point phenomena is either orthogonal or tilted depending on the physical features.

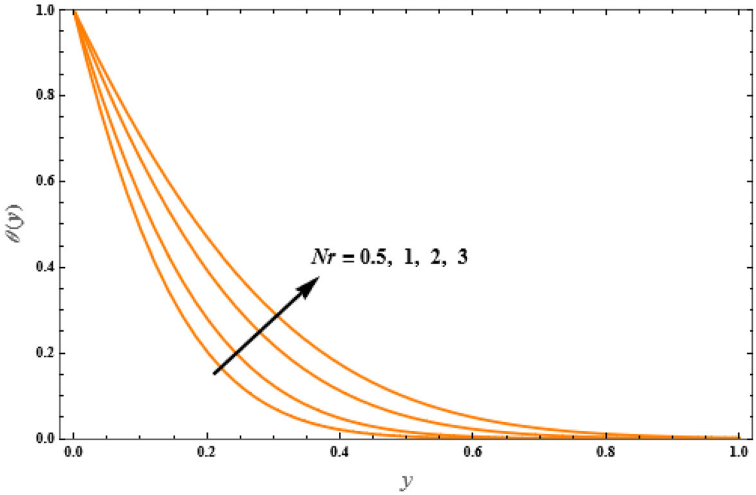

Fig. 9 The impact of N_r on the temperature profile $s = 1$, $\Pr = 6.2$, $\Lambda = 1, A = 1$

- The velocity boundary dropped, by rising the magnitude of the stretching parameter A and Brinkman ratio Λ.
- The thermal boundary layer increases by increasing the thermal radiation N_r.
- In comparison to wall injection, wall suction results in a reduction in the temperature distribution.

Author Contributions USM and AC are responsible for the design and organisation of the research. USM and MR are responsible for the detailed analysis of the work and MR and AC wrote the manuscript. All authors reviewed te manuscript before submission.

Funding There is no funding to declare for this project.

Data Availability Enquiries about data availability should be directed to the authors.

Declarations

Conflict of interest The authors declare no competing interests.

References

1. Choi, S.U.S.: Enhancing thermal conductivity of fluid with nanoparticles. ASME Fluids Eng. Div. **231**, 99–105 (1995)

2. Makinde, O., Animasaun, I.: Thermophoresis and Brownian motion effects on MHD bioconvection of nanofluid with nonlinear thermal radiation and quartic chemical reaction past an upper horizontal surface of a paraboloid of revolution. J. Mol. Liq. **221**, 733–743 (2016)
3. Hayat, T., Aziz, A., Alsaedi, M.T.: A Numerical study for nanofluid flow due to a nonlinear curved stretching surface with convective heat and mass conditions. Results Phys. **7**, 3100–3106 (2017)
4. Das, S., Jana, R.N., Makinde, O.D.: MHD flow of Cu-Al_2O_3/water hybrid nanofluid in porous channel: analysis of entropy generation. Defect Diffusion Forum **377**, 42–61 (2017)
5. Anusha, T., Huang, H., Mahabaleshwar, U.S.: Two dimensional unsteady stagnation point flow of Casson hybrid nanofluid over a permeable flat surface and heat transfer analysis with radiation. J. Taiwan Inst. Chem. Eng. **127**, 79–91 (2021)
6. Aly, E.H., Mahabaleshwar, U.S., Anusha, T., Usafzai, W.K., Pop, I.: Wall jet flow and heat transfer of a hybrid nanofluid subject to suction/injection with thermal radiation. Therm. Sci. Eng. Progress **32**, 101294 (2022)
7. Mahabaleshwar, U.S., Anusha, T., Hatami, M.: The MHD Newtonian hybrid nanofluid flow and mass transfer analysis due to super-linear stretching sheet embedded in porous medium. Sci. Rep. **11**, 22518 (2021)
8. Poornima, T., Sreenivasulu, P., Souayeh, B.: Mathematical study of heat transfer in a stagnation flow of a hybrid nanofluid over a stretching/shrinking cylinder. J. Eng. Phys. Thermophys. **95**, 1443–1454 (2022)
9. Aly, E.H., Pop, I.: MHD flow and heat transfer near stagnation point over a stretching/shrinking surface with partial slip and viscous dissipation: hybrid nanofluid versus nanofluid. Powder Technol. **367**, 192–205 (2020)
10. Shatanawi, T.A.M., Abbas, N., Shatanawi, W.: Mathematical analysis of unsteady stagnation point flow of radiative Casson hybrid nanofluid flow over a vertical riga sheet. Mathematics **10**, 3573 (2022)
11. Jamaludin, A., Naganthran, K., Nazar, R., Pop, I.: MHD mixed convection stagnation point flow of Cu-Al_2O_3/water hybrid nanofluid over a permeable stretching/shrinking surface with heat source/sink. Eur. J. Mech. /B Fluids **84**, 71–80 (2020)
12. Anuar, N.S., Bachok, N., Pop, I.: Influence of MHD hybrid ferrofluid flow on exponentially stretching/shrinking surface with heat source/sink under stagnation point region. Mathematics **9**, 2932 (2021)
13. Hiemenz, K.: Die Grenzschicht an einem in den gleichformigen Flussigkeitsstrom eingetauchten geraden Kreiszylinder. Dingler's Polytech. J. **326**, 321–326 (1911)
14. Wu, Q., Weinbaum, S., Andreopoulos, Y.: Stagnation-point flows in a porous medium. Chem. Eng. Sci. **60**, 123–134 (2005)
15. Weidman, P.D., Mahalingam, S.: Axisymmetric stagnation-point flow impinging on a transversely oscillating plate with suction. J. Eng. Math. **31**, 305–318 (1997)
16. Stuart, J.T.: The viscous flow near a stagnation-point when the external flow has uniform vorticity. J. Aerosp. Sci. Technol. **26**, 124–125 (1959)
17. Hayat, T., Khan, M.I., Farooq, M., Yasmeen, T., Alsaedi, A.: Stagnation point flow with Cattaneo-Christov heat flux and homogeneous-heterogeneous reactions. J. Mol. Liq. **220**, 49–55 (2016)
18. Meraj, M., Hayat, T., Ioan, P., Hendi, A.: Stagnation-point flow and heat transfer of a Casson fluid towards a stretching sheet. Zeitschrift für Naturforschung A **67**, 70–76 (2012)
19. Bhattacharyya, K., Arif, M.G., Pramanik, W.A.: MHD boundary layer stagnation-point flow and mass transfer over a permeable shrinking sheet with suction/blowing and chemical reaction. Acta Tech. **57**, 115 (2012)
20. Merkin, J.H., Pop, I.: Stagnation point flow past a stretching/shrinking sheet driven by Arrhenius kinetics. Appl. Math. Comput. **337**, 583–590 (2018)
21. Zhang, W., Wei, Y., Yu, P., Zhu, Z.: Numerical investigation on buoyancy-driven flow over a circular cylinder in a channel with nonparallel walls. Numer. Heat Transf. Part A Appl. **82**, 299–316 (2022)
22. Mahabaleshwar, U.S., Anusha, T., Hatami, M.: Analysis of a stagnation point flow with hybrid nanoparticles over a porous medium. Fluid Dyn. Mater. Process. **19**, 541–567 (2023)
23. Hsu, C.T.: The Brinkman model for natural convection about a semi-infinite vertical flat plate in a porous medium. Int. J. Heat Mass Transf. **28**, 683–697 (1985)
24. Sneha, K.N., Mahabaleshwar, U.S., Bennacer, R., Ganaoui, M.E.: Darcy Brinkman equations for hybrid dusty nanofluid flow with heat transfer and mass transpiration. Computation **9**, 118 (2021)
25. Zhang, J., Khan, M.I., Al-Khaled, K., El-Zahar, E.R., Acharya, N., Raza, A., Khan, S.U., Xia, W.F., Tao, N.X.: Thermal transport model for Brinkman type nanofluid containing carbon nanotubes with sinusoidal oscillations conditions: a fractional derivative concept. Waves Random Complex Media (2022). https://doi.org/10.1080/17455030.2022.2049926
26. Anusha, T., Mahabaleshwar, U.S., Sheikhnejad, Y.: An MHD of nanofluid flow over a porous stretching/shrinking plate with mass transpiration and brinkman ratio. Transp. Porous Me.d **142**, 333–352 (2022)

27. Bestman, A.R., Adjepong, S.K.: Unsteady hydromagnetic free-convection flow with radiative heat transfer in a rotating fluid. Astrophys. Space Sci. **143**, 73–80 (1998)
28. Sajid, M., Hayat, T.: Influence of thermal radiation on the boundary layer flow due to an exponentially stretching sheet. Int. Commun. Heat Mass Transfer **35**, 347–356 (2008)
29. Sneha, K.N., Mahabaleshwar, U.S., Bhattacharyya, S.: An effect of thermal radiation on inclined MHD flow in hybrid nanofluids over a stretching/shrinking sheet. J. Therm. Anal. Calorim. **148**, 2961–2975 (2023)
30. Lund, L.A., Wakif, A., Omar, Z., Khan, I., Animasaun, I.L.: Dynamics of water conveying copper and alumina nanomaterials when viscous dissipation and thermal radiation are significant: single-phase model with multiple solutions. Math. Methods Appl. Sci. **46**, 11603 (2023)
31. Lund, L.A., Omar, Z., Khan, I., Baleanu, D., Nisar, K.S.: Dual similarity solution of MHD stagnation point flow of Casson fluid with effect of the thermal radiation and viscous dissipation: stability analysis. Sci. Rep. **10**, 15405 (2020)
32. Khan, S.A., Ali, B., Eze, C., Lau, K.T., Ali, L., Chen, J., Zhao, J.: Magnetic dipole and thermal radiation impacts on stagnation point flow of micropolar based nanofluids over a vertically stretching sheet: finite element approach. Processes **9**(7), 1089 (2021). https://doi.org/10.3390/pr90710
33. Maranna, T., Mahabaleshwar, U.S., Kopp, M.I.: The impact of Marangoni convection and radiation on flow of ternary nanofluid in a porous medium with mass transpiration. J. Appl. Comput. Mech. **9**, 487–497 (2023)
34. Turkyilmazoglu, M.: Stagnation-point flow and heat transfer over stretchable plates and cylinders with an oncoming flow: exact solutions. Chem. Eng. Sci. **238**, 116596 (2021)
35. Rosseland, S.: Astrophysik and atom-theoretische Grundlagen. Springer, New York (1931)
36. Umair, K., Zaib, A., Anuar, I., Nepal, C.R., Sakhinah, A.B., Taseer, M., Abdel-Aty, A.H., Ibrahim, S.Y.: Exact solutions for MHD axisymmetric hybrid nanofluid flow and heat transfer over a permeable non-linear radially shrinking/stretching surface with mutual impacts of thermal radiation. Eur. Phys. J. Spcl. Top. **231**, 1195–1204 (2022)